

Freak Waves: Peculiarities of Numerical Simulations

V.E. Zakharov, A.I. Dyachenko, and A.O. Prokofiev

Abstract Numerical simulation of evolution of nonlinear gravity waves is presented. Simulation is done using two-dimensional code, based on conformal mapping of the fluid to the lower half-plane. We have considered two problems: (i) modulation instability of wave train and (ii) evolution of nonlinear Schrödinger equation solitons with different steepness of carrier wave. In both cases we have observed formation of freak waves.

1 Introduction

Waves of extremely large size, alternatively called freak, rogue, or giant waves, are a well-documented hazards for mariners (see, for instance Smith 1976; Dean 1990; Chase 2003). These waves are responsible for loss of many ships and many human lives. Freak waves could appear in any place of the world ocean (see Earle 1975; Mori et al. 2002; Divinsky et al. 2004); however, in some regions they are more probable than in the others. One of the regions where freak waves are especially frequent is the Agulhas current of the South-East coast of South Africa (see Grundlingh 1994; Gutshabash and Lavrenov 1986; Irvine and Tilley 1988; Lavrenov 1998; Mallory 1974). In the paper by Peregrine (1976) it was suggested that in areas of strong current such as the Agulhas, giant waves could be produced when wave action is concentrated by reflection into a caustic region. According to this

V.E. Zakharov

Department of Mathematics, University of Arizona, Tucson, AZ, 857201, USA

and

Waves and Solitons LLC, W. Sereno Dr., Gilbert, AZ, 85233, USA

zakharov@math.arizona.edu

A.I. Dyachenko and A.O. Prokofiev

Landau Institute for Theoretical Physics, 2 Kosygina str., Moscow, 119334, Russia

alex@itp.ac.ru

theory, a variable current acts analogously to an optic lens to focus wave action. The caustic theory of freak waves was supported since that time by works of many authors. Among them were Smith (1976), Gutshabash and Lavrenov (1986), Irvine and Tilley (1988), Sand et al. (1990), Gerber (1987, 1993), Kharif and Pelinovsky (2003). The statistics of caustics along with application to calculation of the freak wave formation probability was studied in the paper of White and Fornberg (1998).

In our opinion, connection between freak wave generation and caustics for swell or wind-driven sea is the indisputable fact. However, this is not the end of the story. Focusing of ocean waves by an inhomogeneous current is a pure linear effect. Meanwhile, there is no doubts that freak waves are essentially nonlinear objects. They are very steep. In the last stage of their evolution, the steepness becomes infinite, forming a “wall of water.” Before this moment, the steepness is higher than that for the limiting Stokes wave. Moreover, a typical freak wave is a single event (see, for instance Divinsky et al. 2004. Before breaking it has a crest, three–four (or even more) times higher than the crests of neighbor waves. The freak wave is preceded by a deep trough or “hole in the sea.” A characteristic life time of a freak wave is short – ten of wave periods or so. If the wave period is 15 s, this is just few minutes. Freak wave appears almost instantly from a relatively calm sea. Sure, these peculiar features of freak waves cannot be explained by a linear theory. Focusing of ocean waves creates only preconditions for formation of freak waves, which is a strongly nonlinear effect.

It is natural to associate appearance of freak waves with the modulation instability of Stoke’s waves. This instability is usually called after Benjamin and Feir; however, it was first discovered by Lighthill (1965). The theory of instability was developed independently by Benjamin and Feir (1967) and by Zakharov (1967). Feir (1967) was the first who observed the instability experimentally in 1967.

Slowly modulated weakly nonlinear Stokes wave is described by nonlinear Schrödinger equation (NLSE), derived by Zakharov (1968). This equation is integrable (see Zakharov and Shabat 1972) and is just the first term in the hierarchy of envelope equations describing packets of surface gravity waves. The second term in this hierarchy was calculated by Dysthe (1979), the next one was found a few years ago by Trulsen and Dysthe (1996). The Dysthe equation was solved numerically by Ablowitz and his collaborates (see Ablowitz et al. 2000, 2001).

Since the first work of Smith (1976), many authors tried to explain the freak wave formation in terms of NLSE and its generalizations, like Dysthe equation. A vast scientific literature is devoted to this subject. The list presented below is long but incomplete: Peregrine (1983); Peregrine et al. (1988), Tanaka (1990), Trulsen and Dysthe (1996), Trulsen and Dysthe (1997), Trulsen (2000), Trulsen et al. (2000), Ablowitz et al. (2000), Onorato et al. (2000, 2001, 2002).

One cannot deny some advantages achieved by the use of the envelope equations. Results of many authors agree to one important point: nonlinear development of modulation instability leads to concentration of wave energy in a small spatial region. On the one hand, this is a “hint” regarding possible formation of freak wave. On the other hand, it is clear that the freak wave phenomenon cannot be explained in terms of envelope equations. Indeed, NLSE and its generalizations are derived by

expansion in series on powers of parameter $\lambda \simeq 1/Lk$, where k is a wave number, L is a length of modulation. For real freak wave $\lambda \sim 1$ and any “slow modulation expansion” fails. However, the analysis in the framework of the NLS-type equations gives some valuable information about formation of freak waves.

Modulation instability leads to decomposition of initially homogeneous Stokes wave into a system of envelope solitons (more accurately speaking, quasi-solitons Zakharov and Kuznetsov (1998); Zakharov et al. (2004)). This state can be called “solitonic turbulence,” or, more exactly “quasisolitonic turbulence.” In the framework of pure NLSE, solitonic turbulence is “integrable.” Solitons are stable, and they scatter on each other elastically. However, even in this simplest scenario, spatial distribution of wave energy displays essential intermittency. More exact Dysthe equation is not integrable. In this model solitons can merge, and this effect increases spatial intermittency and leads to establishing of chaotic intense modulations of energy density. So far this model cannot explain formation of freak waves with $\lambda \sim 1$.

This effect can be explained if the envelope solutions of a certain critical amplitude are unstable and can collapse. In the framework of 1D focusing NLSE solitons are stable; thus solitons instability and the collapse must have a certain threshold in amplitude. Instability of a soliton of large amplitude and further collapse could be a proper theoretical explanation of the freak wave origin.

This scenario was observed in numerical experiment on the heuristic one-dimensional Maida-McLaughlin Tabak (MMT) model (see Majda et al. 1997) of one-dimensional wave turbulence (Zakharov et al. (2004)). At a proper choice of parameters this model mimics gravity waves on the surface of deep water. In the experiments described in the cited paper, instability of a moderate amplitude monochromatic wave leads first to creation of a chain of solitons, which merge due to inelastic interaction into one soliton of a large amplitude. This soliton sucks energy from neighbor waves, becomes unstable, and collapse up to $\lambda \sim 1$, producing the freak wave. We believe that this mechanism of freak wave formation is universal.

The most direct way to prove validity of the outlined above scenario for freak wave formation is a direct numerical solution of Euler equation, describing potential oscillations of ideal fluid with a free surface in a gravitational field. This solution can be made by the methods published in several well-known articles (Dommermuth and Yue (1987); West et al. (1987); Clamond and Grue (2001)). Here we use another method, based on conformal mapping. It should be mentioned that idea to exploit conformal mapping for unsteady flows was presented in Ovsyannikov (1973) and later in Meison et al. (1981), Chalikov and Sheinin (1998). Method used in this article has origin in Dyachenko et al. (1996), has been using in Zakharov et al. (2002), and was finally formulated in Dyachenko (2001). This method is applicable in $1 + 1$ geometry; it includes conformal mapping of fluid bounded by the surface to the lower half-plane together with “optimal” choice of variables, which guarantees well-posedness of the equations (Dyachenko 2005) and existence of smooth, unique solution of the equations for a finite time (Shamin 2006). Here we would like to stress that one of the main goal of this paper is to demonstrate effectiveness of the conformal variables to simulate exact 2D potential flow with a free boundary. Earlier, fully nonlinear numerical experiments regarding wave breaking, freak wave

formation, comparison with weakly nonlinear model (such as Nonlinear Shrodinger equation) were done in the papers Dold and Peregrine (1986), Tanaka (1990), Banner and Tian (1998), Henderson et al. (1999), Clamond and Grue (2002). On the other hand, using conformal approach we have studied in the paper Zakharov et al. (2002) the nonlinear stage of modulation instability for Stokes waves of steepness $\mu = ka \simeq 0.3$ and $\mu = 0.1$.

In the present article we perform similar experiment for waves of steepness $\mu \simeq 0.15$. This experiment could be considered as a simulation of a realistic situation. If a typical steepness of the swell is $0.06 \div 0.07$, in caustic area it could easily be 2–3 times more. In the new experiment, we start with the Stokes wave train, perturbed by a long wave with 20 times less amplitude. We observe development of modulation instability and finally the explosive formation of the freak wave that is pretty similar to waves observed in natural experiments.

2 Basic Equations

Suppose that incompressible fluid covers the domain

$$-\infty < y < \eta(x, t). \quad (1)$$

The flow is potential, hence

$$V = \nabla\phi, \quad \nabla V = 0, \quad \nabla^2\phi = 0. \quad (2)$$

Let $\psi = \phi|_{y=\eta}$ be the potential at the surface and $H = T + U$ be the total energy. The terms

$$T = -\frac{1}{2} \int_{-\infty}^{\infty} \psi \phi_n dx, \quad (3)$$

$$U = \frac{g}{2} \int_{-\infty}^{\infty} \eta^2(x, t) dx \quad (4)$$

are correspondingly kinetic and potential parts of the energy, g is a gravity acceleration, and ϕ_n is a normal velocity at the surface. The variables ψ and η are canonically conjugated; in these variables Euler equation of hydrodynamics reads

$$\frac{\partial \eta}{\partial t} = \frac{\delta H}{\delta \psi}, \quad \frac{\partial \psi}{\partial t} = -\frac{\delta H}{\delta \eta}. \quad (5)$$

One can perform the conformal transformation to map the domain that is filled with fluid

$$-\infty < x < \infty, \quad -\infty < y < \eta(x, t), \quad z = x + iy$$

in z -plane to the lower half-plane

$$-\infty < u < -\infty, \quad -\infty < v < 0, \quad w = u + iv$$

in w -plane. Now, the shape of surface $\eta(x, t)$ is presented by parametric equations

$$y = y(u, t), \quad x = x(u, t),$$

where $x(u, t)$ and $y(u, t)$ are related through Hilbert transformation

$$y = \hat{H}(x(u, t) - u), \quad x(u, t) = u - \hat{H}y(u, t). \quad (6)$$

Here

$$\hat{H}(f(u)) = PV \frac{1}{\pi} \int_{-\infty}^{\infty} \frac{f(u') du'}{u' - u}.$$

Equations (5) minimize the action,

$$S = \int L dt, \quad (7)$$

$$L = \int \psi \frac{\partial \eta}{\partial t} dx - H. \quad (8)$$

Lagrangian L can be expressed as follows,

$$\begin{aligned} L = & \int_{-\infty}^{\infty} \psi (y_t x_u - x_t y_u) du + \frac{1}{2} \int_{-\infty}^{\infty} \psi \hat{H} \psi_u du - \frac{g}{2} \int_{-\infty}^{\infty} y^2 x_u du \\ & + \int_{-\infty}^{\infty} f (y - \hat{H}(x - u)) du. \end{aligned} \quad (9)$$

Here f is the Lagrange multiplier, which imposes the relation (6). Minimization of action in conformal variables leads to implicit equations (see Dyachenko et al. (1996))

$$\begin{aligned} y_t x_u - x_t y_u &= -\hat{H} \psi_u \\ \psi_t y_u - \psi_u y_t + g y y_u + \hat{H}(\psi_t x_u - \psi_u x_t + g y x_u) &= 0. \end{aligned} \quad (10)$$

System (10) can be resolved with respect to the time derivatives. Omitting the details, we present only the final result

$$\begin{aligned} Z_t &= iU Z_u, \\ \Phi_t &= iU \Phi_u - B + ig(Z - u). \end{aligned} \quad (11)$$

Here

$$\Phi = 2\hat{P}\psi \quad (12)$$

is a complex velocity potential, U is a complex transport velocity:

$$U = 2\hat{P} \left(\frac{-\hat{H}\psi_u}{|z_u|^2} \right) \quad (13)$$

and

$$B = \hat{P} \left(\frac{|\Phi_u|^2}{|z_u|^2} \right) = \hat{P} (|\Phi_z|^2). \quad (14)$$

In (12), (13), and (14) \hat{P} is the projector operator generating a function that is analytical in a lower half-plane

$$\hat{P}(f) = \frac{1}{2} (1 + i\hat{H}) f.$$

In (11)

$$z(w) \rightarrow w, \quad \Phi(w) \rightarrow 0, \quad \text{at } v \rightarrow -\infty.$$

All functions z , Φ , U , and B are analytic ones in the lower half-plane $v < 0$.

Recently, we found that (11) were derived in Ovsyannikov (1973), and we call them here Ovsyannikov's equations, OE. Implicit equations (10) were not known until 1994, so we call them DKSZ-equations.

Note, (10) can be used to obtain the Lagrangian description of surface dynamics. Indeed, from (10) one can get

$$\Psi = \partial^{-1} \hat{H} (y_t x_u - x_t y_u). \quad (15)$$

Plugging (15) to (8) one can express Lagrangian L only in terms of surface elevation. This result was independently obtained by Balk (1996). In Dyachenko (2001) (11) were transformed to a simple form, which is convenient both for numerical simulation and analytical study. By introducing new variables

$$R = \frac{1}{Z_w}, \quad V = i\Phi_z = i\frac{\Phi_w}{Z_w} \quad (16)$$

one can transform system (11) into the following one:

$$\begin{aligned} R_t &= i(UR_w - RU_w), \\ V_t &= i(UV_w - RB_w) + g(R - 1). \end{aligned} \quad (17)$$

Now complex transport velocity U and B

$$\begin{aligned} U &= \hat{P}(V\bar{R} + \bar{V}R), \\ B &= \hat{P}(V\bar{V}). \end{aligned} \quad (18)$$

Thereafter, we call (17) and (18) Dyachenko equations, DE.

Both DKSZ-equations (10) and OE (11) have the same constants of motion

$$H = - \int_{-\infty}^{\infty} \Psi \hat{H} \Psi_u du + \frac{g}{2} \int_{-\infty}^{\infty} y^2 x_u dy, \quad (19)$$

the same total mass of fluid

$$M = \int_{-\infty}^{\infty} y x_u du, \quad (20)$$

and the same horizontal momentum

$$P_x = \int_{-\infty}^{\infty} \Psi y_u \, du. \quad (21)$$

The Dyachenko equations (17) and (18) have the same integrals. To express them in terms of R and V , one has to perform the integration

$$Z = u + \int_{-\infty}^u \frac{du}{R}, \quad \Phi = -i \int_{-\infty}^u \frac{V}{R} \, du. \quad (22)$$

3 Numerical Instability with Respect to Small Scale Perturbation

The problem of stability of the equations of motion of the fluid with a free surface goes back to the famous work of Taylor (1950). He has found the relationship between the growth rate of the interface instability, the wave-length of the perturbation, and the gravity acceleration. Today we would say that Taylor instability is the manifestation of the ill-posedness of the Cauchy problem for the case when gravity acceleration is directed out of the fluid.

The problem of well-posedness of the Cauchy problem for the potential irrotational flows with a free surface was studied in many papers. First time it was studied by Nalimov in Nalimov (1974).

3.1 Instability of Φ - Z Equations

Let us consider (11) with (13) and (14). Stability of the large-scale solution with respect to short-scale perturbation will be considered. Let this large-scale solution have subscripts 0, namely, $\Phi_0(w, t)$ and $Z_0(w, t)$. Obviously, perturbed solution is the following:

$$\Phi = \Phi_0 + \delta\Phi, \quad Z = Z_0 + \delta Z. \quad (23)$$

Characteristic wavenumber k of $\delta\Phi$ and δZ is much larger than characteristic wavenumber k_0 of Φ_0 and Z_0 . Let us expand arguments of U and B in (13 and 14) up to the first order in $\delta Z'$ and $\delta\Phi'$:

$$\begin{aligned} \frac{i\Phi'}{Z'\bar{Z}'} + \text{c.c.} &\simeq \frac{i\Phi'_0}{Z'_0\bar{Z}'_0} + (\bar{\Phi}'_0 - \Phi'_0) \frac{i\delta Z'}{Z_0'^2\bar{Z}'_0} + \frac{i\delta\Phi'}{\bar{Z}'_0 Z'_0} + \text{c.c.} \\ \frac{\Phi'}{Z'} \frac{\bar{\Phi}'}{\bar{Z}'} &\simeq \frac{\Phi'_0 \bar{\Phi}'_0}{Z'_0 \bar{Z}'_0} - \frac{\Phi'_0 \bar{\Phi}'_0}{Z'_0 \bar{Z}'_0} \frac{\delta Z'}{Z'_0} + \frac{\bar{\Phi}'_0 \delta\Phi'}{\bar{Z}'_0 Z'_0} + \text{c.c.} \end{aligned} \quad (24)$$

Now we can calculate U and B :

$$\begin{aligned} U &\simeq U_0 + \frac{i}{Z_0'^2 \bar{Z}_0'} (\bar{\Phi}'_0 - \Phi'_0) \delta Z' + \frac{i \delta \Phi'}{\bar{Z}'_0 Z_0'}, \\ B &\simeq B_0 - \frac{\Phi'_0 \bar{\Phi}'_0}{Z_0' \bar{Z}'_0} \frac{\delta Z'}{Z_0'} + \frac{\bar{\Phi}'_0}{Z_0' \bar{Z}'_0} \delta \Phi'. \end{aligned} \quad (25)$$

When deriving (25) we have to calculate projector of (24). To do this we deal with products like $A_0 \delta Z'$ and $A_0 \delta \bar{Z}'$. It is easy to see that due to the scale separation of A_0 and δZ the following relations are valid:

$$\begin{aligned} \hat{P}(A_0 \delta Z') &\simeq A_0 \delta Z', \\ \hat{P}(A_0 \delta \bar{Z}') &\simeq 0. \end{aligned} \quad (26)$$

Now we are ready to write down the linearized equations for perturbations.

$$\begin{aligned} \delta Z_t &= i \left(U_0 - \frac{i}{Z_0' \bar{Z}'_0} (\Phi'_0 - \bar{\Phi}'_0) \right) \delta Z' - \frac{\delta \Phi'}{\bar{Z}'_0}, \\ \delta \Phi_t &= \frac{\Phi_0'^2}{Z_0'^2 \bar{Z}'_0} \delta Z' + i \left(U_0 + \frac{i(\Phi'_0 + \bar{\Phi}'_0)}{Z_0' \bar{Z}'_0} \right) \delta \Phi' + ig \delta Z. \end{aligned} \quad (27)$$

Now we treat all functions with subscript \dots_0 in (27) as constants. This is so-called ‘‘method of frozen coefficient,’’ which is widely used in analysis of numerical schemes.

Let δZ and $\delta \Phi \sim \exp(i\omega t - ikx)$. Then the following dispersion relation can be derived:

$$\omega = kV_D \pm \sqrt{gk \frac{1}{\bar{Z}'_0}}. \quad (28)$$

Here V_D has a meaning of Doppler frequency shift and is equal to

$$V_D = \frac{\Psi'_0}{Z_0' \bar{Z}'_0} - \hat{H} \frac{\hat{H} \Psi'_0}{Z_0' \bar{Z}'_0}. \quad (29)$$

So, from (28) immediately follows that for gravity waves ω has imaginary part, which grows as a function of k :

$$\gamma = \frac{1}{2} \sqrt{gk} \frac{\eta'_x}{\sqrt{X'}}.$$

It means that large scale solution is unstable with respect to the perturbation.

This instability takes place only in the numerics when dealing with Ovsyannikov equations.

3.2 Stability of R - V Equations

Doing similar analysis for R - V equations one can easily derive the following set of equations for perturbations:

$$\begin{aligned}\delta R_t &= V_D \delta R' - i|R_0|^2 \delta V' + b_{11} \delta R + b_{12} \delta V, \\ \delta V_t &= V_D \delta V' + b_{21} \delta R + b_{22} \delta V,\end{aligned}\quad (30)$$

with

$$\begin{aligned}b_{11} &= -i(U'_0 + R_0 \bar{V}'_0 - R'_0 \bar{V}_0), \\ b_{12} &= i(\bar{R}_0 R'_0 - R_0 \bar{R}'_0), \\ b_{21} &= g + i(\bar{V}_0 V'_0 - B'_0) = g + \tilde{g}, \\ b_{22} &= i(\bar{R}_0 V'_0 - R_0 \bar{V}'_0).\end{aligned}\quad (31)$$

Coefficient $b_{21} = g + \tilde{g}$ is pure real. Indeed,

$$\begin{aligned}\tilde{g} - \bar{\tilde{g}} &= i(\bar{V}_0 V'_0 - B'_0 + V_0 \bar{V}'_0 - \bar{B}'_0), \\ &= i \frac{\partial}{\partial u} (V_0 \bar{V}_0 - B_0 - \bar{B}_0) = 0.\end{aligned}$$

Applying “method of frozen coefficient” one can obtain the following dispersion relation:

$$\omega = kV_D + i\Omega \pm \frac{1}{|Z'_0|} \sqrt{(g + \tilde{g})k - \Omega^2}.\quad (32)$$

while

$$\begin{aligned}\Omega &= \frac{i}{2} \left(\frac{\bar{V}'_0}{Z'_0} - \frac{V'_0}{\bar{Z}'_0} \right), \\ \tilde{g} &= i(\bar{V}_0 V'_0 - B'_0).\end{aligned}$$

Note, V_D , Ω , and \tilde{g} are pure real values.

Although ω in (32) has imaginary part, *it doesn't grow as a function of k* (of course, if \tilde{g} does not exceed g). This property makes the system of equation (17) numerically stable with respect to small scale perturbation.

4 Freak Waves as a Result of Modulation Instability

Here we study modulation instability of uniform wave train of Stokes wave numerically. For time integration the standard Runge–Kutta method of the fourth order was used.

Question of great interest is the nonlinear stage of the instability. Here and everywhere below we do simulation in periodic domain $L = 2\pi$ and

$$g = 1.$$

Wavetrain of the amplitude a with wavenumber k_0 is unstable with respect to large scale modulation δk . Growth rate of the instability γ is

$$\gamma = \frac{\omega_0}{2} \left(\left(\frac{\delta k}{k_0} \right)^2 (ak_0)^2 - \frac{1}{4} \left(\frac{\delta k}{k_0} \right)^4 \right)^{\frac{1}{2}}. \quad (33)$$

Here ω_0 is the linear dispersion relation for gravity wave

$$\omega_0 = \sqrt{gk_0}.$$

- The shape of Stokes progressive wave is given by

$$y = \frac{c^2}{2g} \left(1 - \frac{1}{|Z_u|^2} \right),$$

while Φ is related to the surface as

$$\Phi = -c(Z - u), \quad V = ic(R - 1).$$

The amplitude of the wave h/L is the parameter for initial condition. (For the sharp peaked limiting wave $h/L \simeq 0.141$).

- Put 100 such waves with small perturbation in the periodic domain of 2π .

In such a way we prepared initial wave train with the steepness $\mu \simeq 0.095$. Main Fourier harmonic of this wave train is $k = 100$. Similar problem was studied in Song and Banner (2002). But instead of long wavetrain they studied evolution of small group of waves.

For perturbation small value for Fourier harmonic with $k_p = 1$ was set. So, that

$$R_k = R_k^{\text{unperturbed}} + 0.05R_{100} \exp^{-ik_p u}.$$

Surface profile of this initial condition is shown in Fig. 1.

Fourier spectrum of the initial condition is shown in Fig. 2.

After sufficient large time, which is more than 1,300 wave periods, one can observe freak wave formation, as it is shown in Fig. 3. Freak wave grows from mean level of waves to its maximal value for several wave periods, than vanishes or breaks.

Detailed view at the freak wave at the moment of maximal amplitude is shown in Fig. 4. This set of experiments is similar to that of Dold and Peregrine (1986), Tanaka (1990). The difference is that we were able to increase the accuracy of the simulation, and consider much longer wavetrains. Also (due to using conformal mapping) we can simulate breaking with multivalued surface profile. Accuracy in the simulation is very important because the freak wave appears in a very subtle

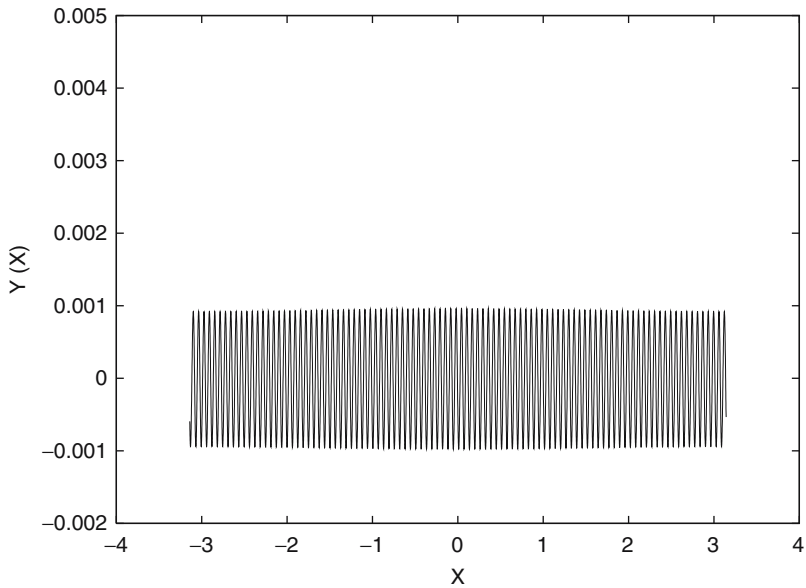


Fig. 1 Initial profile of the wave train

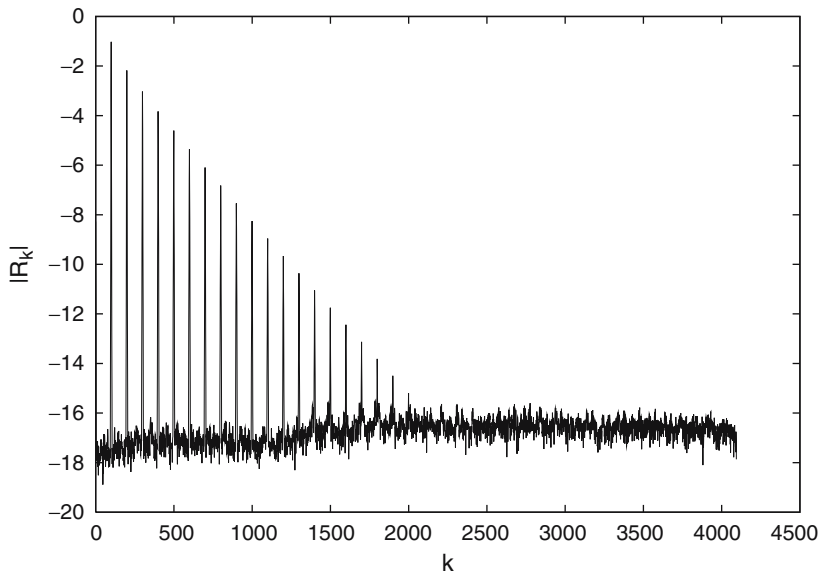


Fig. 2 Fourier coefficients $|R_k|$ for initial condition ($\mu \simeq 0.095$)

manner on the phase relations between Fourier harmonics of the surface. Moreover, for shorter wavetrains, threshold of modulation instability increases and breaking does not happen even for large steepness. In our experiments we have observed

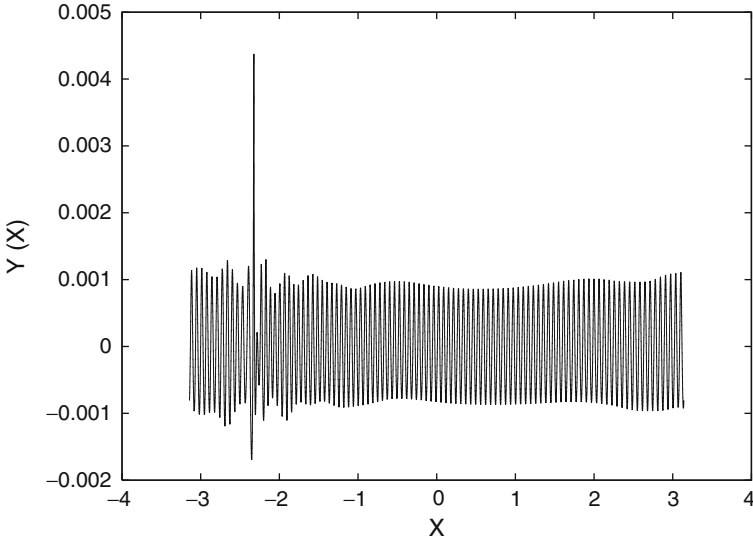


Fig. 3 Freak wave on the surface profile. $T = 802.07$

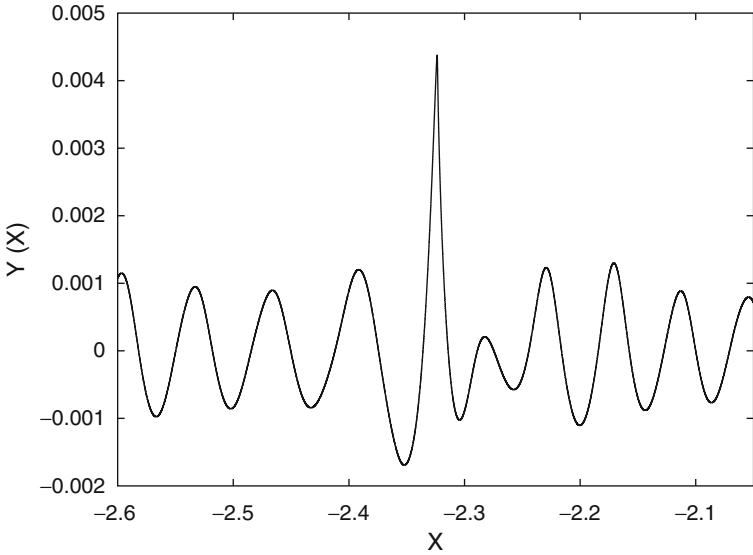


Fig. 4 Zoom in surface profile at $T = 802.07$

threshold of steepness for wave breaking a little less than in Tanaka (1990), but above $\mu = 0.1$. Still, surface profile from Tanaka (1990) (Fig. 5) is very similar to the picture in Fig. 4 with $\mu = 0.095$.

During numerical simulation of the final stage of freak wave formation, resolution must be increased to resolve high curvature of the surface profile. To do this we

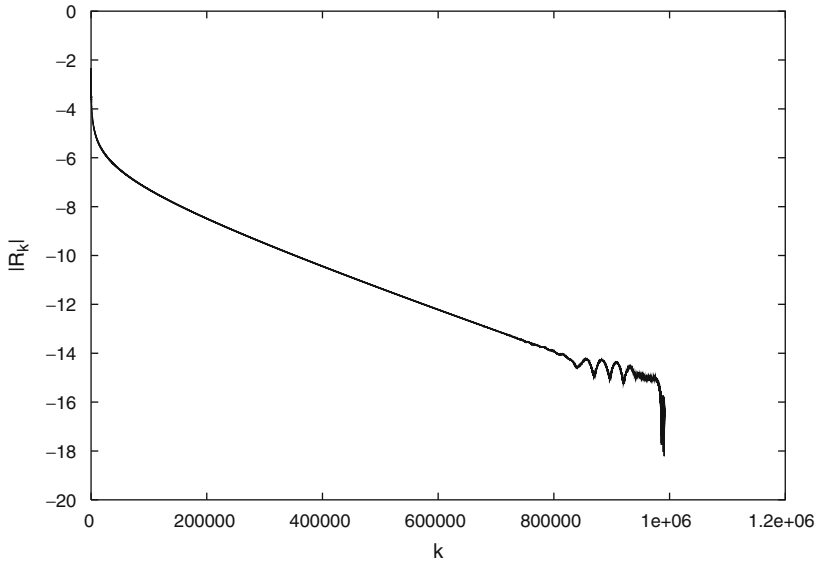


Fig. 5 Fourier coefficients $|R_k|$ at $T = 802.07$

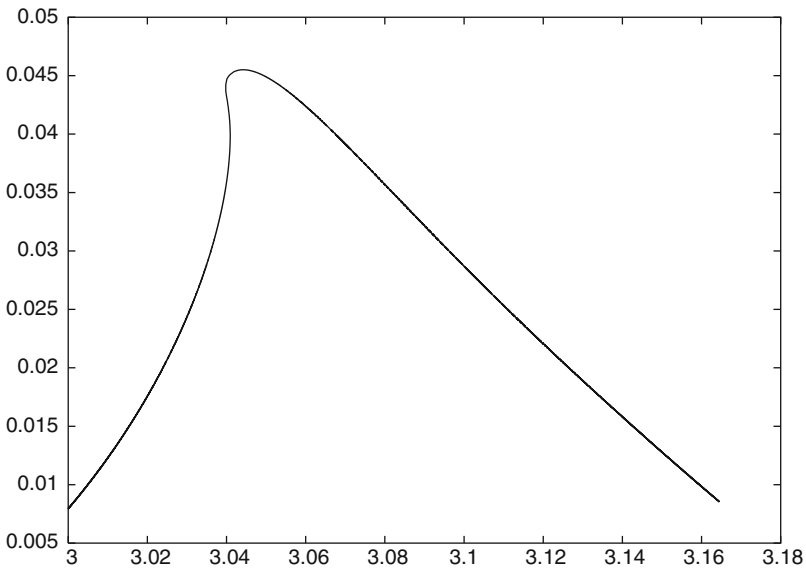


Fig. 6 Profile of breaking wave

have been increasing number of Fourier harmonics, which reached 2^{20} at the end ($T = 802.07$). Fourier coefficients of R_k are shown in Fig. 5.

If amplitude of the wave train is large, then freak wave may eventually break. Such a picture is presented in the Fig. 6, which corresponds to the other numerical simulation with the initial steepness $\mu \simeq 0.14$.

5 Exact Equations and Nonlinear Shrödinger Approximation

Evolution of weakly nonlinear Stokes wavetrain can be described by nonlinear Shrödinger equation (*NLSE*), derived by Zakharov (1968). This equation is integrable (see Zakharov and Shabat 1972) and is just the first term in the hierarchy of envelope equations describing packets of surface gravity waves. The second term in this hierarchy was calculated by Dysthe (1979), the next one was found a few years ago by Trulsen and Dysthe (1996). The Dysthe equation was solved numerically by Ablovitz and his collaborates (see Ablovitz et al. 2000).

Since the first work of Smith (1976), many authors tried to explain the freak wave formation in terms of NLSE and its generalizations, like Dysthe equation. A vast scientific literature is devoted to this subject. The list presented below is long but incomplete: Ablovitz et al. (2000), Onorato et al. (2000, 2001, 2002), Peregrine (1983); Peregrine et al. (1988), Trulsen and Dysthe (1996, 1997), Trulsen (2000), Trulsen et al. (2000), Clamond and Grue (2002).

One cannot deny some advantages achieved by the use of the envelope equations. Results of many authors agree in one important point: nonlinear development of modulation instability leads to concentration of wave energy in a small spatial region. This is a “hint” regarding possible formation of freak wave. On the other hand, it is clear that the freak wave phenomenon cannot be explained in terms of envelope equations. Indeed, NLSE and its generalizations are derived by expansion in series on powers of parameter $\lambda \simeq 1/Lk$, where k is a wave number and L is a length of modulation. For real freak wave $\lambda \sim 1$ and any slow modulation expansion fails. At this point interesting question rises: what happens to NLSE approximation when increasing the steepness of the carrier wave? In particular, we study “exact” soliton solutions for NLSE placed in the exact equations (17).

Such type of problem was considered in the Henderson et al. (1999), but with low resolution, and small length of periodic carrier. Also in Clamond and Grue (2002) numerical solutions for envelope equation was compared with “almost” exact equations.

For (17) NLSE model can be derived for the envelope of R .

$$R = 1 + R_1 e^{-ik_0 u - \omega_0 t} + \dots$$

$$iR_{1t} + \frac{1}{8} \frac{\omega_0}{k_0^2} R_{1uu} + \frac{1}{2} \omega_0 k_0^2 |R_1|^2 R_1 = 0.$$

Initial conditions consist of “linear wave carrier” $e^{-ik_0 u}$, modulated in accordance with soliton solution for NLSE:

$$R(u) = 1 + s_0 \frac{e^{-ik_0 u}}{\cosh(\lambda k_0 u)},$$

$$V(u) = -ic_0 s_0 \frac{e^{-ik_0 u}}{\cosh(\lambda k_0 u)}. \quad (34)$$

Here s_0 is the steepness of the carrier wavetrain, c_0 is the phase velocity of the carrier.

First comparison of fully nonlinear model for water wave with NLSE was done in Clamond and Grue (2002) for the wave carrier with the steepness $\mu \simeq 0.091$. For such steepness there was a good agreement between two models, but only for the short time. After finite time weakly nonlinear model (*NLSE*) ceases to be valid.

In our work we want to study the situation with larger and smaller steepness to find out how NLSE approximation breaks.

5.1 Small Steepness

First experiment was intended to observe how NLSE works. In the initial conditions (34) we used

$$s_0 \simeq 0.07, \quad \lambda = 0.1, \quad k_0 = 100.$$

Initial surface of fluid is shown in Fig. 7.

After couple of thousands wave periods, soliton changes a little as it is seen in Fig. 8. Also in the Figs. 9 and 10 Fourier spectra of the soliton at both moments of time are presented.

So, one can see that for the steepness $\mu \leq 0.07$ NLSE model is quite reasonable.

Another numerical experiment showing effective simulation with (17) along with applicability NLSE model for moderate steepness, $\mu \simeq 0.085$, is the collision of two solitons.

In Fig. 11 initial condition is shown. Moment of collision is shown in the Fig. 12 and detailed view showing carrier wavetrain under the envelope is in the Fig. 13.

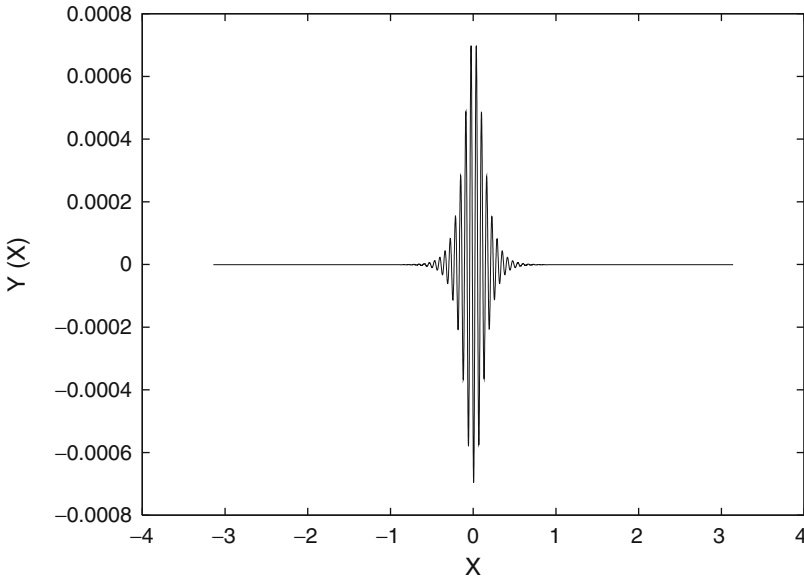


Fig. 7 Initial surface profile like for NLSE soliton with $\mu \simeq 0.07$

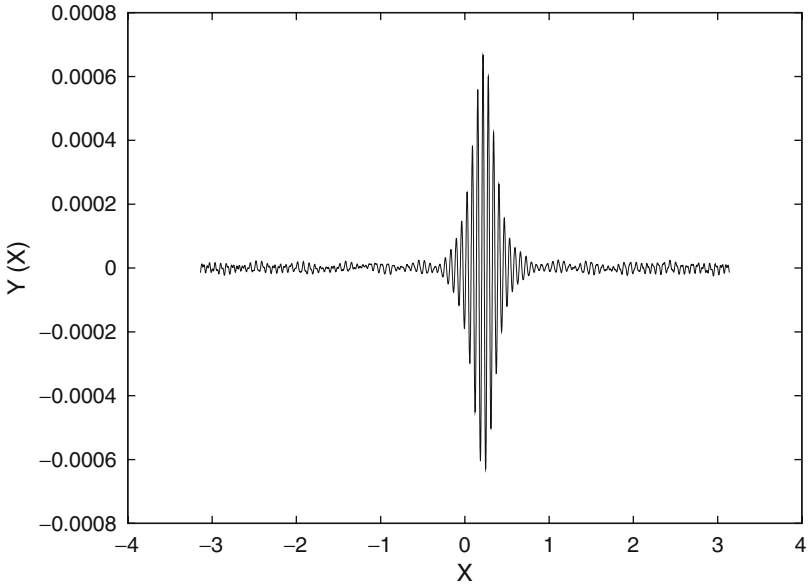


Fig. 8 Surface profile like for NLSE soliton with $\mu \simeq 0.07$ at $T = 1,500$

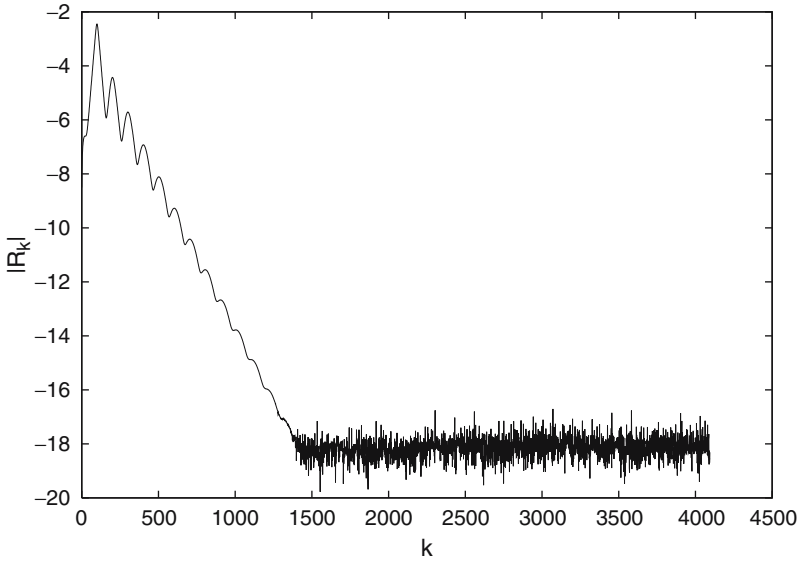


Fig. 9 Fourier harmonics of the initial soliton with $\mu \simeq 0.07$

After second collision (recall that boundary conditions are periodic) solitons are plotted in Fig. 14. Fourier spectra of these two solitons at the moments of time $T = 0.05, 30.8,$ and 250.0 are shown in Figs. 15–17.

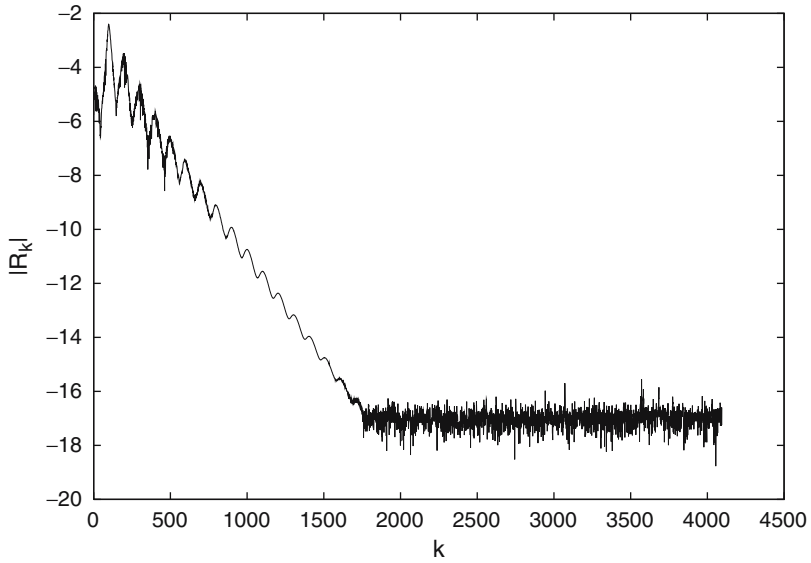


Fig. 10 Fourier harmonics of the soliton with $\mu \simeq 0.07$ at $T = 1,500$

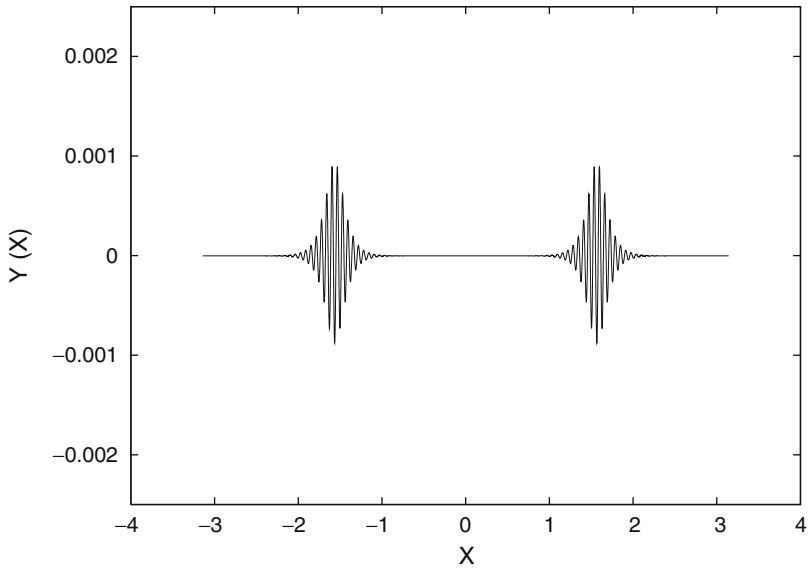


Fig. 11 Initial surface profile of two NLSE solitons with $\mu \simeq 0.085$

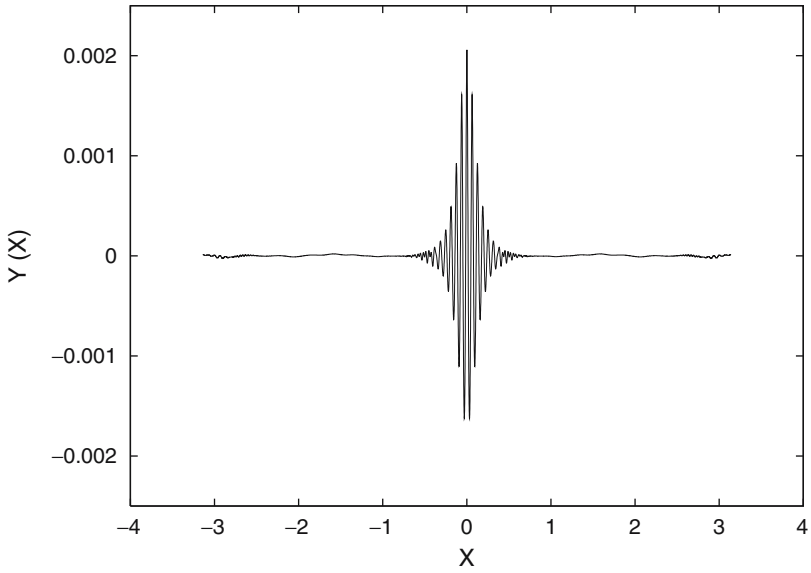


Fig. 12 Two NLSE solitons with $\mu \simeq 0.085$, collide at $T = 30.8$

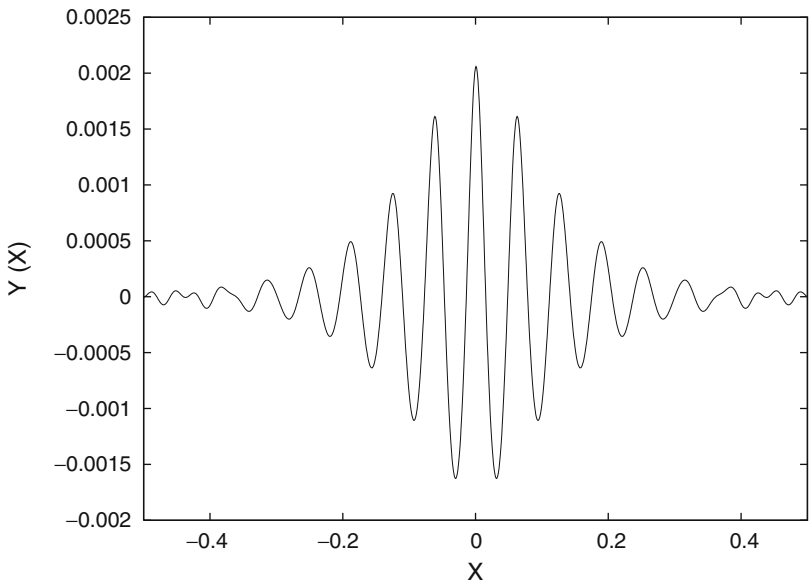


Fig. 13 Detailed view of two colliding NLSE solitons with $\mu \simeq 0.085$ at $T = 30.8$

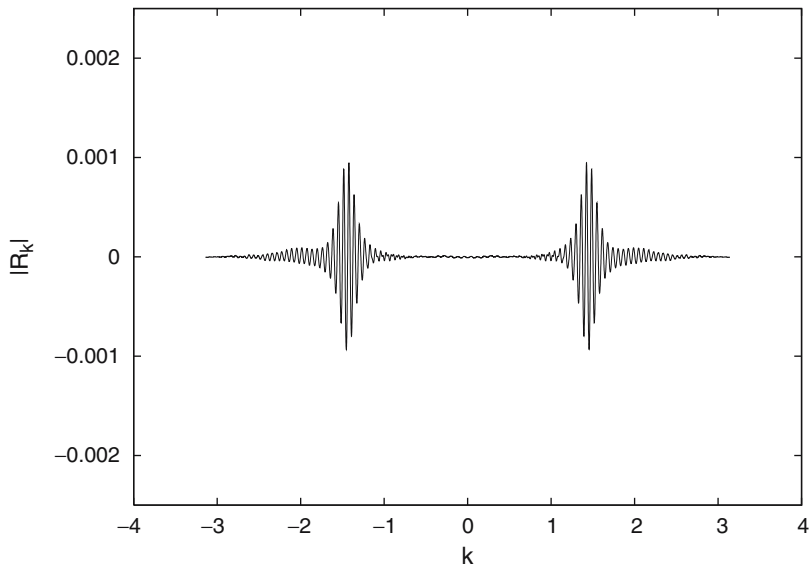


Fig. 14 Two *NLSE* solitons with $\mu \simeq 0.085$ after two collisions at $T = 250.0$

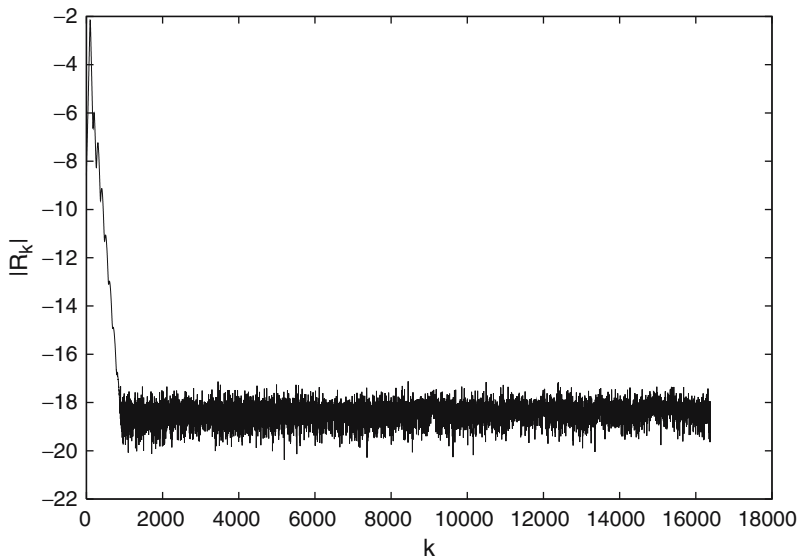


Fig. 15 Fourier spectrum of the initial surface profile of two *NLSE* solitons with $\mu \simeq 0.085$

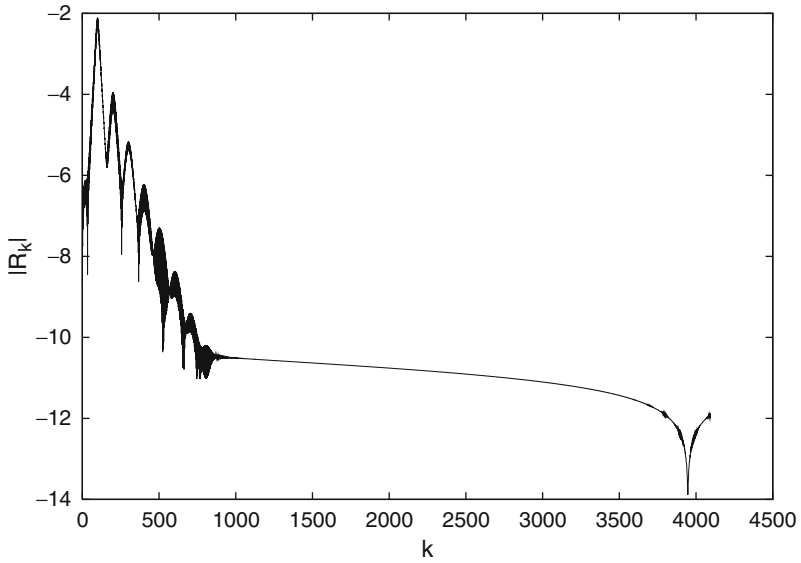


Fig. 16 Fourier spectrum of two colliding NLSE solitons with $\mu \simeq 0.085$ at $T = 30.8$

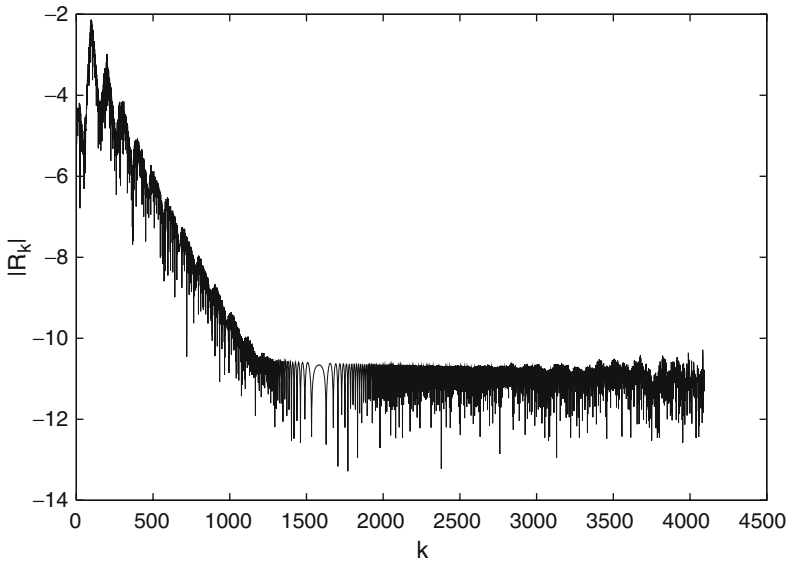


Fig. 17 Fourier spectrum of two NLSE solitons with $\mu \simeq 0.085$ at $T = 250.0$

5.2 Large Steepness

Now let us turn to the higher steepness of the carrier,

$$\mu = 0.1.$$

In the Fig. 18 there is initial condition. Again, after couple of thousand wave periods, soliton changes a little as it is seen in Fig. 19. In Figs. 20 and 21 Fourier spectra of the soliton at both moments of time are presented.

From this pictures one can see that for steepness $\mu \simeq 0.10$ some corrections to the NLSE model are desirable. Dysthe equations are exactly intended for that situation.

But what happens when further increasing the steepness? Below we consider the case of the steepness of the carrier

$$\mu = 0.14.$$

In the Fig. 22 there is initial condition. Very fast, after couple of dozen wave periods, soliton drastically changes as it is seen in Fig. 23. One can see freak wave at the surface (in Fig. 24). In the Figs. 25 and 26 Fourier spectra of the soliton at both moments of time are presented. They demonstrate the quality of the numerical simulation. The tail of the spectrum in Fig. 26 shows that the resolution decreases (aliasing errors “go up”); however, the simulation remains stable.

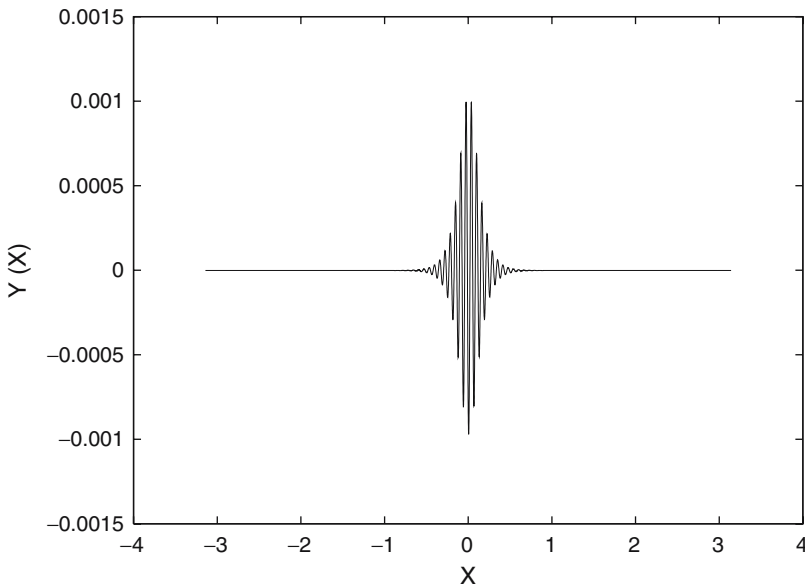


Fig. 18 Initial surface profile like for NLSE soliton with $\mu \simeq 0.10$

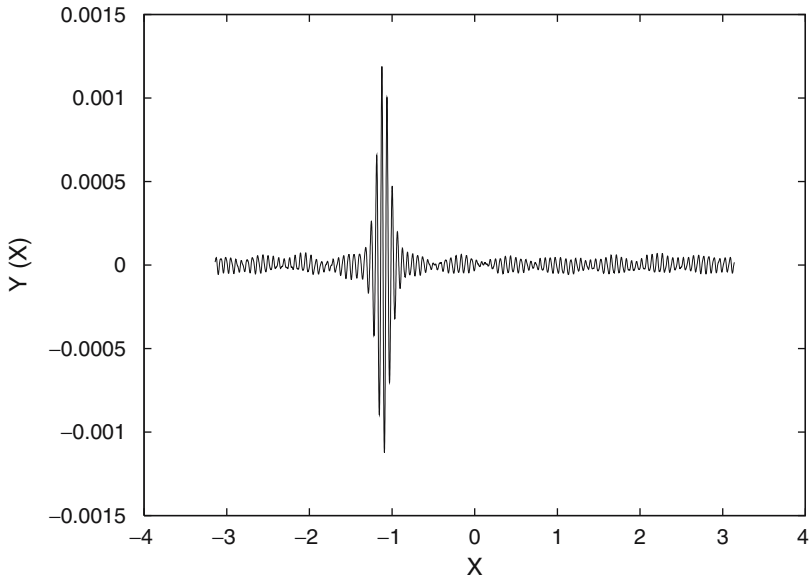


Fig. 19 Surface profile like for NLSE soliton with $\mu \simeq 0.10$ at $T = 2,345$

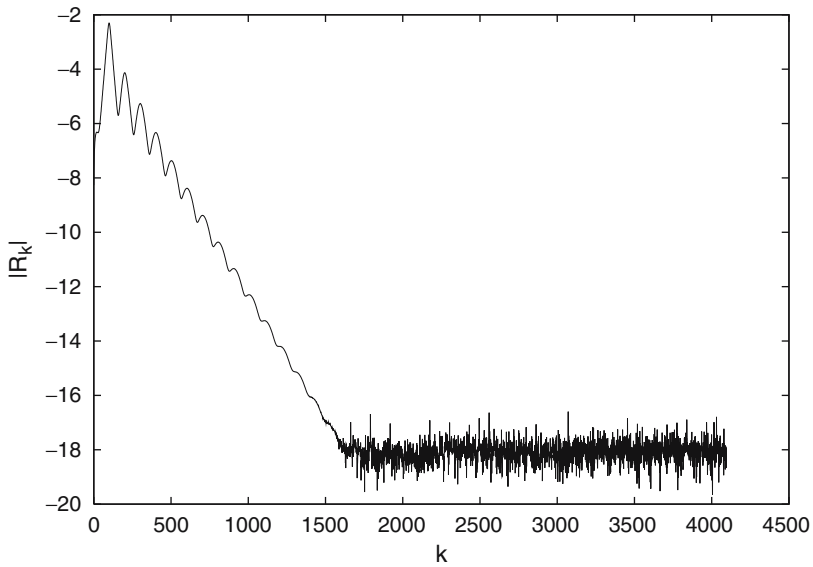


Fig. 20 Fourier harmonics of the initial soliton with $\mu \simeq 0.10$

From the last case, with the steepness $\mu = 0.14$, one can see that envelope approximation completely fails. Such event as one single crest (freak wave) can not be described in terms of wave envelope.

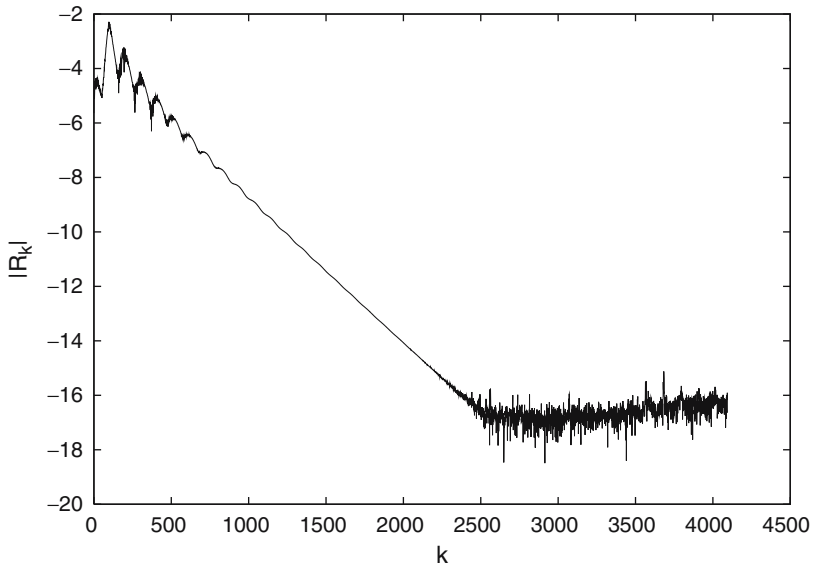


Fig. 21 Fourier harmonics of the soliton with $\mu \simeq 0.10$ at $T = 2,345$

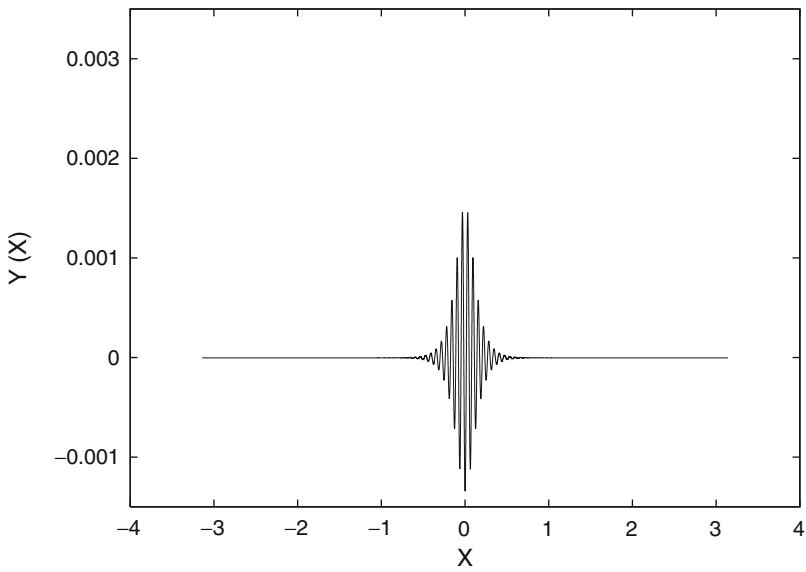


Fig. 22 Initial surface profile like for NLSE soliton with $\mu \simeq 0.14$

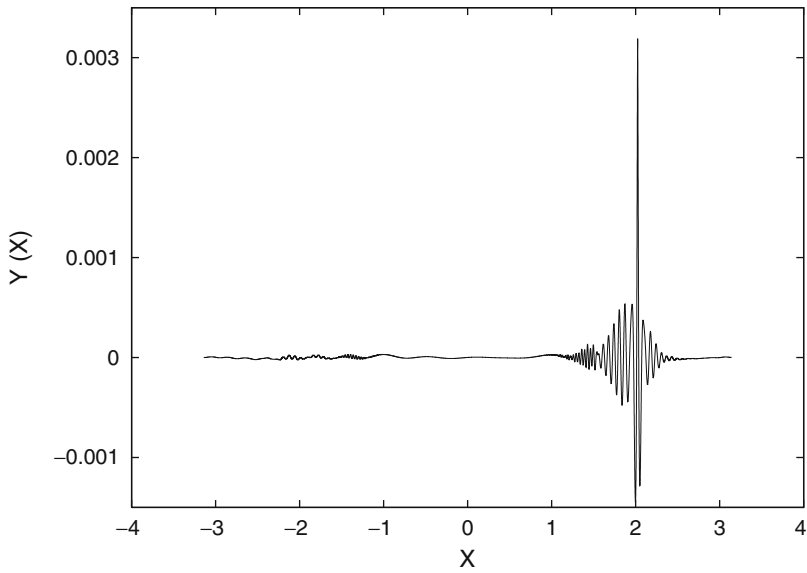


Fig. 23 Surface profile like for NLSE soliton with $\mu \simeq 0.14$ at $T = 38.4$

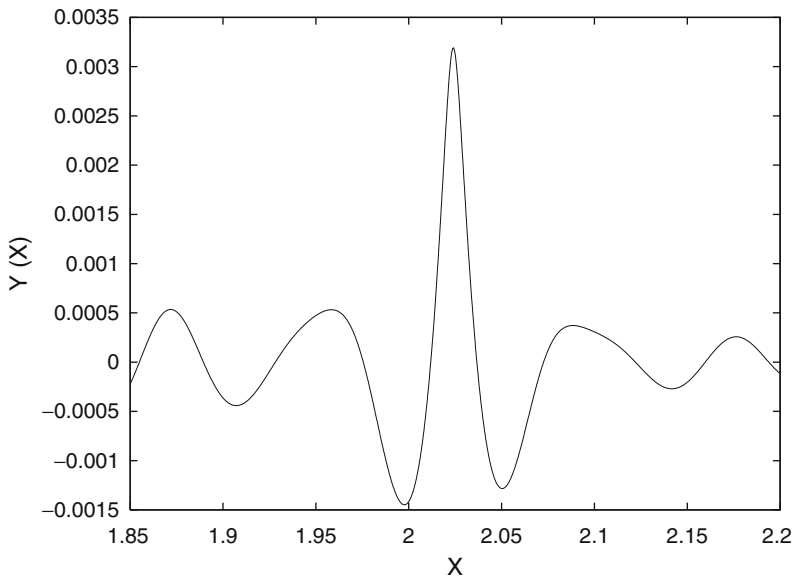


Fig. 24 Zoomed surface profile near freak wave $\mu \simeq 0.14$ at $T = 38.4$

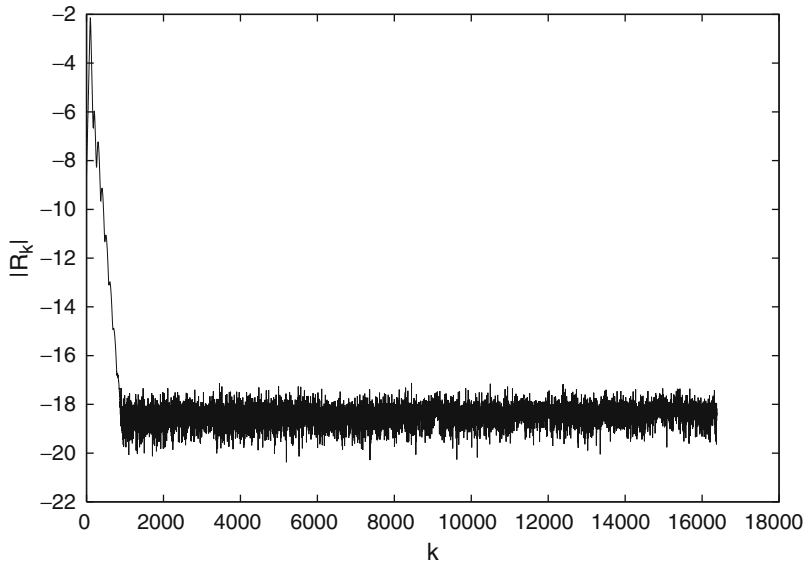


Fig. 25 Fourier harmonics of the initial soliton with $\mu \simeq 0.14$

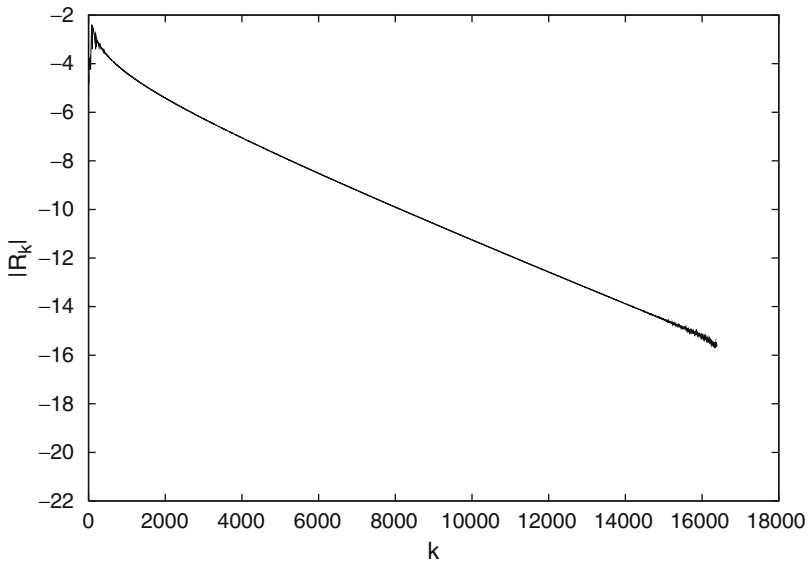


Fig. 26 Fourier harmonics of the soliton with $\mu \simeq 0.14$ at $T = 38.4$

6 Do Freak Waves Appear from Quasisolitonic Turbulence?

Let us summarize the results of our numerical experiments. Certainly, they reproduce the most apparent features of freak waves: single wave crests of very high amplitude, exceeding the significant wave height more than three times, appear from “nowhere” and reach full height in a very short time, less than ten periods of surrounding waves. The singular freak wave is preceded by the area of diminished wave amplitudes. Nevertheless, the central question about the physical mechanism of freak waves origin is still open.

In our experiments, the freak wave appears as a result of development of modulation instability, and it takes a long time for the onset of instability to create a freak wave. Indeed, the level of perturbation in our last experiment is relatively high. The 2–3 inverse growth-rate is enough to reach the state of full-developed instability, when the initial Stokes wave is completely decomposed. Meanwhile, the freak wave appears only after 15th inverse growth-rates of instability. What happens after developing of instability but before formation of freak wave?

During this relatively long period of time, the state of fluid surface can be characterized as quasisolitonic turbulence, which consists of randomly located quasi-solitons of different amplitudes moving with different group velocities. Numerical study of interaction of envelope soliton was done in Clamond and Grue (2002). Such interaction leads to formation of wave with large amplitude. Here we can think in terms of quasisolitonic turbulence. Such turbulence was studied in the recent work of Zakharov et al. (2004) in a framework of so-called defocusing MMT model:

$$i \frac{\partial \Psi}{\partial t} = \left| \frac{\partial}{\partial x} \right|^{1/2} \Psi + \left| \frac{\partial}{\partial x} \right|^{3/4} \left(\left| \frac{\partial}{\partial x} \right|^{3/4} \Psi \right)^2 \left| \frac{\partial}{\partial x} \right|^{3/4} \Psi. \quad (35)$$

This is a heuristic model description of gravity surface waves in deep water. In this model, quasi-solitons of small amplitude are stable, interact inelastically, and can merge. Above some critical level quasi-solitons of large amplitude are unstable. They collapse in finite time forming very short wave pulses, which can be considered as models of freak waves. Equation 35 has the exact solution:

$$\begin{aligned} \Psi &= A e^{ikx - i\omega t} \\ \omega &= k^{1/2} \left(1 + k^{5/2} A^2 \right). \end{aligned} \quad (36)$$

This solution can be constructed as a model of the Stokes wave and is unstable with respect to modulation instability. Development of this instability was studied numerically. On the first stage, the unstable monochromatic wave decomposes to a system of almost equal quasi-solitons. Then, the quasi-solitonic turbulence is formed: quasi-solitons move chaotically, interact with each other, and merge. Finally they create one large quasi-soliton, which exceeds threshold of instability and collapses, creating a freak wave.

One can think that a similar scenario of freak wave formation is realized in a real sea. We like to stress that the key point in this scenario is the quasi-solitonic turbulence and not the Stokes wave. The Stokes wave is just a “generator” of this turbulence. The quasisolitonic turbulence can appear as a result of instability of narrow spectral distributions of gravity waves.

The formulated above concept is so far a hypothesis, which has to be confirmed by future numerical experiments.

Acknowledgments This work was supported by the US Army Corps of Engineers Grant W912BU-07-P-0231, by ONR Grant N00014-06-C-0130, by NSF Grant DMS 0404577, by RFBR Grant 06-01-00665, 07-01-92165, by the Program “Fundamental Problems in Nonlinear Dynamics” from the RAS Presidium, and by Grant “Leading Scientific Schools of Russia.”

References

- Ablovitz MI, Hammack D, Henderson J, Scholder CM (2000) Modulated periodic stokes waves in deep water. *Phys Rev Lett*:887–890
- Ablovitz MI, Hammack D, Henderson J, Scholder CM (2001) Long-time dynamics of the modulational instability of deep water. *Phys D* 152–153:416–433
- Balk A (1996) A Lagrangian for water waves. *Phys Fluids* 8:416–420
- Banner M, Tian X (1998) On the determination of the onset of wave breaking for modulating surface gravity waves. *J Fluid Mech* 367:107–137
- Benjamin TB, Feir JE (1967) The disintegration of wave trains on deep water: Part 1. Theory. *J Fluid Mech* 27:417–430
- Chase(2003) <http://bell.mma.edu/achase/NS-221-Big-Wave.html>
- Chalikov D, Sheinin D (1998) Direct modeling of one-dimensional nonlinear potential waves. In: Perrie W (ed) *Nonlinear ocean waves: Advances in fluid mechanics*, vol 17. Computation Mechanics Publications, MA, pp 89–110
- Clamond D, Grue J (2001) A fast method for fully nonlinear-wave computations. *J Fluid Mech* 447:337–355
- Clamond D, Grue J (2002) Interaction between envelope solitons as a model for freak wave formation: Part 1. Long time interaction. *C.R.Mecanique* 330:575–580
- Dean RG (1990) Freak waves: A possible explanation. In: Torum A, Gudmestad OT (eds) *Water wave kinetics*. Kluwer, Dordrecht, pp 609–612
- Divinsky VD, Levin BV, Lopatikhin LI, Pelinovsky EN, Slyunyaev AV (2004) A freak wave in the Black sea: Observations and simulation. *Doklady Earth Sci* 395:438–443
- Dold JW (1992) An efficient surface integral algorithm applied to unsteady gravity waves. *J Comput Phys* 103:90–115
- Dold JW, Peregrine DH (1986) Water-wave modulation. In: *Proceedings of 20th International Conference on Coastal Engineering*, vol 1, Chap 13, pp 163–175
- Dommermuth DG, Yue DKP (1987) A high-order spectral method for the study of nonlinear gravity waves. *J Fluid Mech* 184:267–288
- Dyachenko AI, Kuznetsov EA, Spector MD, Zakharov VE (1996) Analytical description of the free surface dynamics of an ideal fluid (canonical formalism and conformal mapping). *Phys Lett A* 221:73–79
- Dyachenko AI (2001) On the dynamics of an ideal fluid with free surface. *Doklady Math* 63:115–118
- Dyachenko AI, Zakharov VE (2005) Modulation instability of stokes wave - Freak wave. *JETP Lett* 81(6):255–259

- Dyachenko AI (2005) Instability in the numeric models of free surface hydrodynamics. In: International conference on Frontiers of Nonlinear Physics, St.Petersburg-Nizhny Novgorod, Russia, 2–9 August 2005
- Dysthe KB (1979) Note on a modification to the nonlinear Schrodinger equation for application to deep water waves. Proc R Soc Lond Ser A 369:105–114
- Earle MD (1975) Extreme wave conditions during Hurricane Camille. J Geophys Res 80:377–379
- Feir JE (1967) Discussion: Some results from wave pulse experiments. Proc R Soc Lond A 299:54–58
- Gerber M (1987) The Benjamin-Feir instability of a deep water s tokens wave packet in the presence of a non-uniform medium. J Fluid Mech 176:311–332
- Gerber M (1993) The interaction of deep water gravity waves and an annular current: Linear theory. J Fluid Mech 248:153–172
- Grundlingh ML (1994) Evidence of surface wave enhancement in the southwest Indian Ocean from satellite altimetry. J. Geophys. Res. 99:7917–7927
- Gutshabash YS, Lavrenov IV (1986) Swell transformation in the Cape Agulhas current. Izv Atmos Ocean Phys 22 494–497
- Henderson KLD, Peregrine DH, Dold JW (1999) Unsteady water wave modulations: Fully nonlinear solutions and comparison with nonlinear Schrodinger equation. Wave Motion 29:341–361
- Irvine DE, Tilley DG (1988) Ocean wave directional spectra and wave-current interaction in the Agulhas from the shuttle imaging radar-B synthetic aperture radar. J Geophys Res 93:15389–15401
- Kharif C, Pelinovsky E (2003) Physical mechanisms of the rogue wave phenomena. Eur J Mech B: Fluids 22:603–634
- Lavrenov IV (1998) The wave energy concentration at the Agulhas current of South Africa. Nat Hazards 17:117–127
- Lighthill M.J. (1965) Contribution to the theory of waves in nonlinear dispersive systems. J Inst Math Appl 1:269–306
- Majda A, McLaughlin D, Tabak A (1997) one-dimensional model for dispersive wave turbulence. J Nonlinear Sci 7:9–44
- Mallory JK (1974) Abnormal waves on the south-east of South Africa. Inst Hydrog Rev 51:89–129
- Meison D, Orzag S, Izraeli M (1981) Applications of numerical conformal mapping. J Comput Phys 40:345–360
- Mori N, Liu PC, Yasuda T (2002) Analysis of freak wave measurements in the sea of Japan. Ocean Eng 29:41399–41414
- Nalimov VI (1974) The Cauchy-Poisson problem. (Russian) Dinamika Sploshnoi Sredy, Vyp. 18. Dinamika Zidkost. so Svobod Granicami:104–210
- Onorato M, Osborne AR, Serio M, Damiani T (2001) Occurrence of freak waves from envelope equation in random ocean wave simulations. In: Olagnon M, Athanassoulis GA (eds) Rogue waves 2000: Brest, France, Ifremer, pp 181–192
- Onorato M, Osborne AR, Serio M (2000) The nonlinear dynamics of rogue waves and holes in deep-water gravity wave trains. Phys Lett A 275:386–393
- Onorato M, Osborne AR, Serio M, Bertone S (2001) Freak waves in random oceanic sea states. Phys Rev Lett 86:5831–5834
- Onorato M, Osborne AR, Serio M (2002) Extreme wave events in directional, random oceanic sea states. Phys Fluids 14:L25–L28
- Ovsyannikov LV (1973) Dinamika sploshnoi sredy, M.A. Lavrent'ev Institute of hydrodynamics Sib. Branch USSR Acad Sci, No.15, pp 104–125
- Peregrine DH (1976) Interaction of water waves and currents. Adv Appl Mech 16:9–117
- Peregrine DH (1983) Water waves, nonlinear Schrodinger equations and their solutions. J Aust Math Soc B 25:16–43

- Peregrine DH, Skynner D, Stiassnie M, Dold N (1988) Nonlinear effects on focused water waves. In: Proceedings of 21th international conference on coastal engineering, vol 1, chap 54, pp 732–742
- Sand SE, Hansen NE, Klitting P, Gudmestad OT, Sterndorff MJ (1990) Freak wave kinematics. In: Torum A, Gudmestad OT (eds) Water wave kinematics, Kluwer, Dodrecht, pp 535–549
- Shamin RV (2006) On the existence of smooth solutions to the Dyachenko equations governing free-surface unsteady ideal fluid flows. Doklady Math 73(1):112–113
- Smith, R. Giant waves, Fluid Mech. 77 (1976), 417–431
- Song J, Banner ML (2002) On determining the onset and strength of breaking for deep water waves: Part 1. Unforced irrotational wave groups. J Phys Oceanogr 32:2541–2558
- Tanaka M (1990) Maximum amplitude of modulated wavetrain. Wave Motion 12:559–568
- Taylor G (1950) The Instability of liquid surfaces when accelerated in a direction perpendicular to their Planes. I. Proc R Soc Lond A 201:192–196
- Trulsen K, Dysthe KB (1996) A modified nonlinear Schrodinger equation for broader bandwidth gravity waves on deep water. Waves Motion 24:281–289
- Trulsen K, Dysthe KB (1997) Freak waves – A three-dimensional wave simulation. In: Proceedings of 21st symposium on naval hydrodynamics, 1997, pp 550–558 <http://www.nap.edu/books/0309058791/html/550.html>
- Trulsen K (2001) Simulating the spatial evolution of a measured time series of a freak wave. In: Olagnon M, Athanassoulis GA (eds) Rogue waves 2000: Brest, France, November 2000, Ifremer, pp 265–274
- Trulsen K, Kliakhandler I, Dysthe KB, Velarde MG (2000) On weakly nonlinear modulation of waves on deep water. Phys Fluids 12:2432–2437
- West B, Brueckner K, Janda R, Milder D, Milton R (1987) A new numerical method for surface hydrodynamics. J Geophys Res C 92(11):11803–11824
- White BS, Fornberg B (1998) On the chance of freak waves at sea. J Fluid Mech 355:113–138
- Zakharov VE (1967) Stability of nonlinear waves in dispersive media. J Teor Prikl Fiz 51 (1966) 668–671 (in Russian); Sov Phys JETP 24:455–459
- Zakharov VE (1968) Stability of periodic waves of finite amplitude on a surface of deep fluid. J Appl Mech Tech Phys 9:190–194
- Zakharov VE, Shabat AB (1972) Exact theory of two-dimensional self-focusing and one-dimensional self-modulation of waves in nonlinear media. Sov Phys JETP 34:62–69
- Zakharov VE, Kuznetsov EA (1998) Optical solitons and quasisolitons. JETP 86:1035–1046
- Zakharov VE, Dyachenko AI, Vasilyev OA (2002) New method for numerical simulation of non-stationary potential flow of incompressible fluid with a free surface. Eur J Mech B Fluids 21:283–291
- Zakharov VE, Dias F, Pushkarev AN (2004) One-dimensional wave turbulence. Phys Rep 398: 1–65